

Case study of testing different materials for seat belt retractor torsion bar by the means of finite element analysis

Bogdan Ioan NITULEASA , Alexandru Ionut RADU *, Dana Luca MOTOC 

Faculty of Mechanical Engineering, Transilvania University of Braşov, Braşov, Romania

*Corresponding author: alexandru.radu@unitbv.ro

Keywords

FEA
torsion bar
material comparison
seat belt

Abstract

This paper examines the use of various materials for the force limiter torsion bar found in an automotive seat belt assembly. We have selected the following materials: carbon steel, cast stainless steel, cast low alloy steel and cast aluminium alloy. The primary method used for this study is finite element analysis (FEA) and the use of the named materials on a 3D model of the torsion bar, constructed using the dimensions of a standard part. The 3D models were created with a 3D CAD program and the FEA analysis was carried out with special software. For the input values, the torsion bar was fixed at one corner and a 360 degree rotation shift at the other corner. A fine mesh of 1.5 mm/element was also set to get a more accurate analysis. The results of this study are in the form of stress, strain, safety factor and displacement plots generated by the FEA analysis software showing the difference between the materials. The main outcome of the study is to determine the best overall material to manufacture the part in terms of performance and cost.

History

Received: 10-12-2022

Revised: 28-12-2022

Accepted: 29-12-2022

1. Introduction

Passive vehicle safety is crucial for the safety of occupants in car accidents [1]. The seat belt keeps the occupant in the seat without the risk of secondary impacts between the occupant's body and the vehicle interior [2]. Usually, the loads acting on the vehicle occupants are generated by the deceleration of the vehicle and are also limited by the body movement against the seat [3].

The most common type of seat belt system is the three-point belt system with a roller retractor, belt tensioner and torsion bar as a force limiter [4]. In fatal accidents, 75 % of the vehicle occupants were thrown out of the car in the crash [5]. Seat belts have also been shown to reduce the risk of injury by up to 70 % [6]. The role of the force limiter is to release the occupant after the impact to reduce the effects of the pretensioner system which can damage the occupant's torso

[7]. In almost all cases, the force limiter is a torsion bar which, when triggered by the occupant's body movement (after impact), responds with a torque value and loosens the seat belt a few inches. The torque value is around 50 – 60 Nm and will deform the rod as it only needs to be used once.

The material from which this part is made is crucial to its functionality [8]. Typically, it is made of plain carbon steel with high yield strengths to deform from torque but not break. Software testing is used to pre-calculate and evaluate automotive parts before they are manufactured and installed in vehicles [9,10]. Typically, a method called finite element analysis (FEA) is used to evaluate a vehicle part. This method uses a complex algorithm and 3D models to assign materials and apply different loads to the parts to determine the stress and strain values of the part [11-14].

In the automotive industry, there is a tendency to reduce the weight of parts in order to reduce the overall weight of the vehicle. This is called lightweight and is achieved by using lighter weight



This work is licensed under a Creative Commons Attribution-NonCommercial 4.0 International (CC BY-NC 4.0) license

composite materials for some high-strength parts [15,16].

This study aims to use different materials for the torsion bar and compare the results applied using a finite element analysis and a CAD model. The result would reflect what would be an optimal material to use based on structural performance, weight and cost. The torsion bar chosen for this study works by holding one end still and twisting the other end [17]. In the finite element study, a moment is applied at one end to create a torque load to simulate rotary motion [18]. The materials tested were carbon steel, cast stainless steel, cast low alloy steel and cast aluminium alloy.

2. Used methods

The method used was a finite element analysis using dedicated software and a 3D CAD model designed from an existing torsion bar. The torsion bar dimensions are shown in Figure 1.

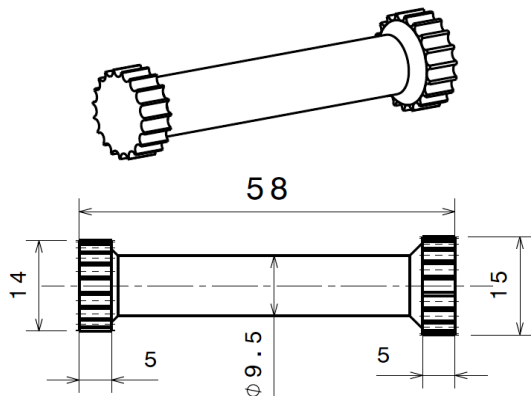


Figure 1. Torsion bar dimensions

The torsion bar is mounted in the seat belt spool retractor and when deployed releases the spool with a 360 degree rotation. The coil and torsion bar assembly are shown in Figure 2.

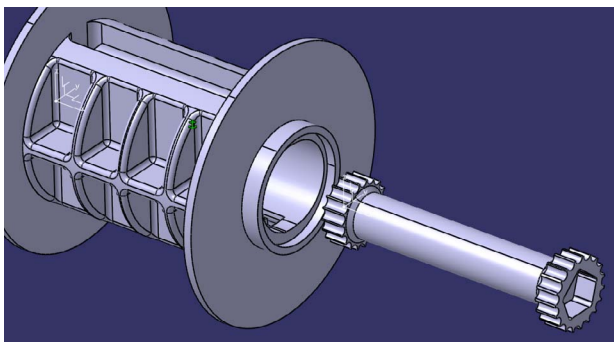


Figure 2. Spool and torsion bar assembly

In the finite element analysis, only the torsion bar was used to simplify the process and to get a

better result because only the torsion bar will be given a moment.

2.1 Material description

The material used is shown in Table 1 [19]. The property values of the materials were obtained from the FEA software database. Interesting material properties are the yield point and the tensile strength, but also the modulus of elasticity, which gives the material its elasticity, a property that is essential for the torsion bar.

Table 1. Material properties

Material	Modulus of elasticity, MPa	Tensile strength, MPa	Yield strength, MPa
Carbon steel AISI 1030	2.1×10^5	459.5	338.2
Cast stainless steel ASTM CB30	2.0×10^5	651.8	412.6
Cast low alloy steel AISI 4335M	2.0×10^5	1236	1205
Cast aluminium alloy AA 319.0	7.4×10^5	246	164.8

Also, the price of each material was studied from an economic point of view to determine which material is the most cost-effective to produce the part from. Prices are shown in Table 2 [20,21].

Table 2. Material cost

Material	Cost, USD/kg
Carbon steel AISI 1030	1
Cast stainless steel ASTM CB30	1.5
Cast low alloy steel AISI 4335M	2.5
Cast aluminium alloy AA 319.0	5.8

2.2 FEA configuration of the model

For the simulation to have a realistic representation of part load, the analysis was conducted using a mode called explicit dynamics, instead of a structural study [22]. In this mode, if the part breaks, it would be shown in a graphical representation. In the FEA analysis software, the 3D model was imported and a cylindrical coordinate system was set in order to add an angular displacement on the Y axis (green arrow) as seen in Figure 3.

The next step was to create the mesh of the part and for a better analysis; the size of the mesh

step was set to 1.5 mm. The mesh model is presented in Figure 4.

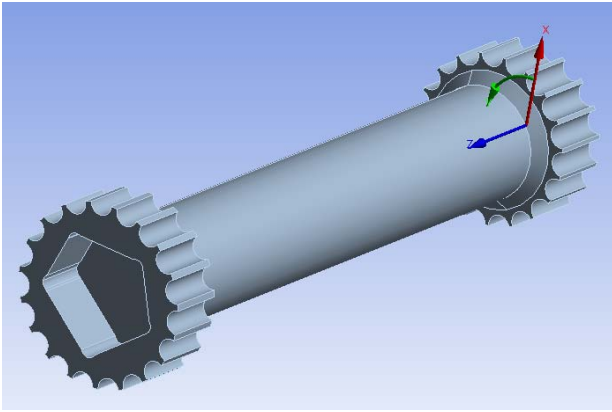


Figure 3. Torsion bar model with the cylindrical coordinate system

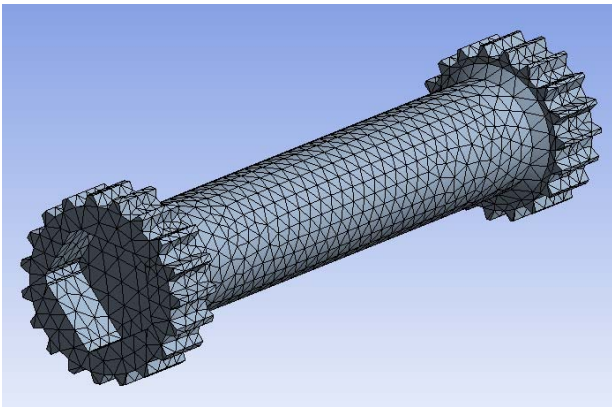


Figure 4. Mesh model of the torsion bar

At one end of the model, a fixed support was added to keep the part solid and at the other end, a displacement was introduced on the Y axis (Fig. 5).

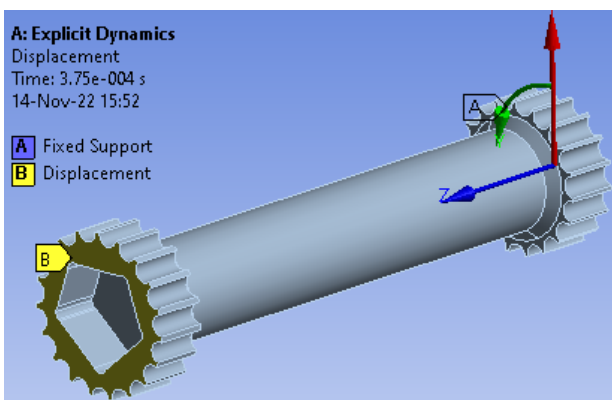


Figure 5. Fixed support and displacement of part

For this study, we simulated the model with a displacement of 360 degree angle, or one complete rotation of the torsion bar, using a nonlinear solver called *Ansys Autodyn*. Also, the simulation end time was set to 0.000375 s. This is an optimal setting used in the simulation software

in order to obtain the desired results in a short period of time.

Each material affects the mass of the part as well. This is important due to the tendency to reduce weight in automotive parts while keeping the strength of the material [23]. In Table 3, the weight, volume and density of the torsion bar are presented for each material used.

Table 3. Torsion bar weight for each material

Material	Weight, g	Volume, cm ³	Density, g/cm ³
Carbon steel AISI 1030	36.1	4.6	7.85
Cast stainless steel ASTM CB30	34.6		7.525
Cast low alloy steel AISI 4335M	36.0		7.825
Cast aluminium alloy AA 319.0	12.9		2.796

3. Results

The results of the study are in form of a graphical representation of the stress areas on the model for each material simulated. In Figure 6, the equivalent stress results are shown for the carbon steel. The results show a maximum value of 716 MPa in the area with the most load (marked in red) and with an average of around 480 MPa on the other end. The maximum value surpassed the yield strength of the material, but that was to be expected because this part deforms while under load in order to function as a force limiter.

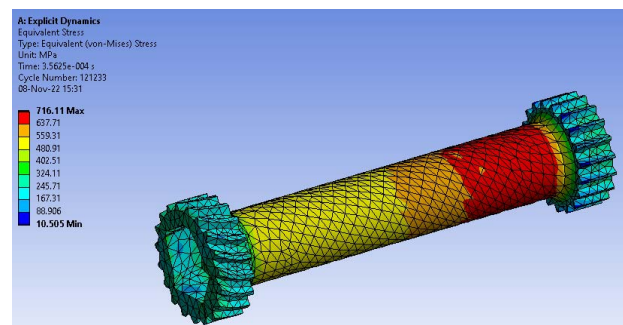


Figure 6. Stress results for carbon steel

In Figure 7, the stress results are presented for the cast stainless steel material. In this case, the maximum value obtained was 1197 MPa, with an average stress of 930 MPa. Because this material has higher strengths than carbon steel, we see higher values, but with a lower maximum in the torsion area.

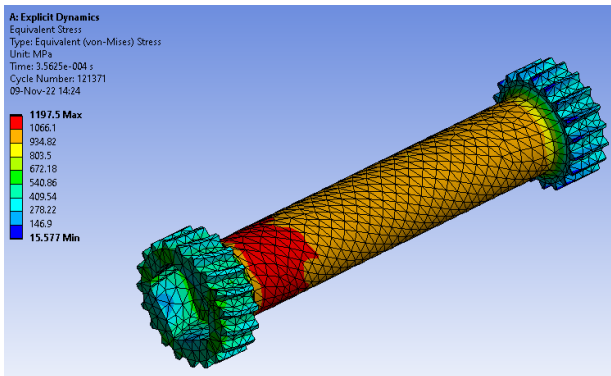


Figure 7. Stress results for cast stainless steel

In Figure 8, the stress results are presented for cast low alloy steel. The maximum stress value obtained was 1725 MPa, all around the centre part of the torsion bar. This result is expected because this material has the highest values of tensile and yield strengths.

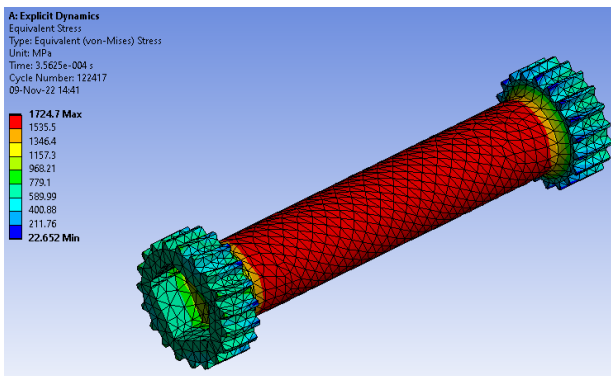


Figure 8. Stress results for cast low alloy steel

The fourth material, cast aluminium alloy, is presented in Figure 9. The result maximum value was 1412 MPa, around the centre part of the torsion bar, but more on the applied moment part. Even though this material has the lowest tensile and yield strength, it does have the highest modulus of elasticity which means it has the most elasticity and this translates to a deformation without breaking the torsion bar.

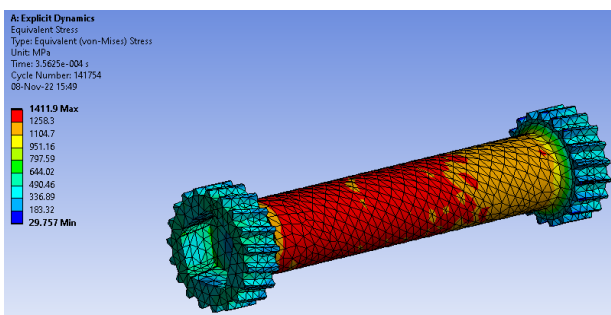


Figure 9. Stress results for cast aluminium alloy

To better understand the materials, a plot has been generated with the maximum equivalent

stress represented as a function of time. This is presented in Figure 10. The stress results show that carbon steel achieved the lowest overall stress value, followed by cast stainless steel. The low alloy steel had the highest stress value, over 1000 MPa, while the carbon steel had the lowest value of 500 MPa. This result shows that carbon steel has better resistance to stress over a longer period of time.

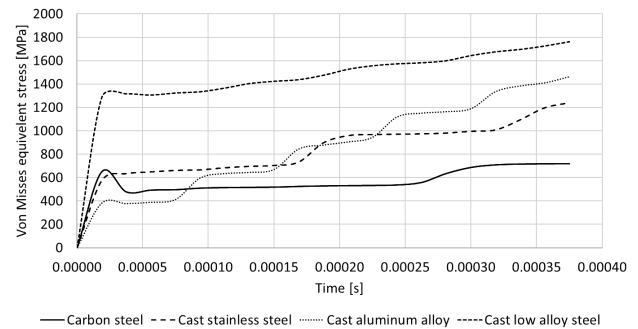


Figure 10. Maximum values of stress equivalent test

Figure 11 shows the average values of the stress test. The average values of the materials share a similar pattern to the maximum ones, but the range is lower, as expected due to the fact in some areas of the part, the stress level is low.

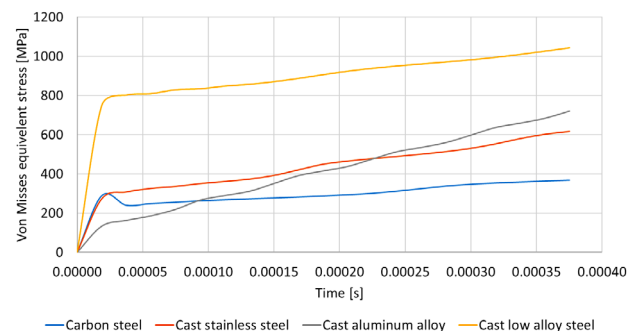


Figure 11. Average values of stress equivalent test

In Figure 12, the maximum strain test values are presented. The results of the strain test show that the maximum deformation ratio of the cast aluminium alloy was the highest at 0.018 mm/mm and carbon steel had the lowest value of 0.002 mm/mm. In Figure 13, the average strain values are presented. The average results value shows a similar pattern to the maximum ones, but with a lower ratio.

By obtaining the strain and stress values of each material, a comparison of the stress in regards to strain was obtained and presented in Figure 14. If we consider the shear values for the materials, we can plot the shear stress in regards to the equivalent stress and this is presented in Figure 15.

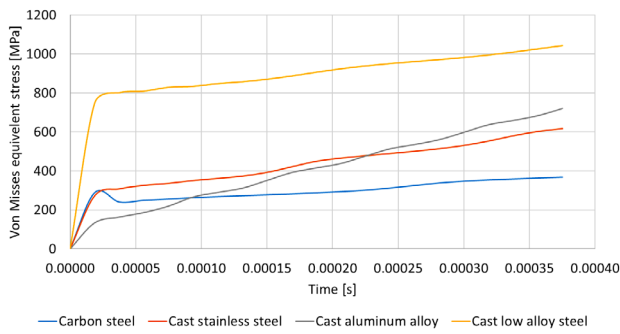


Figure 12. Maximum values of strain test

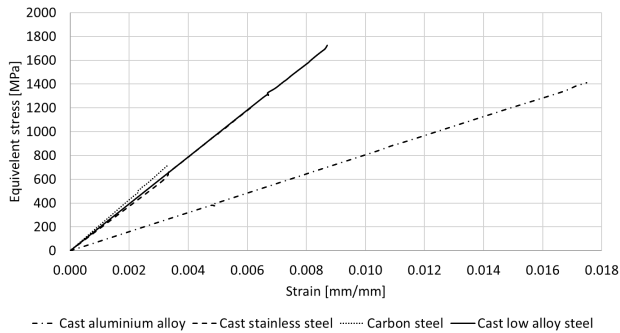


Figure 14. Strain vs. stress diagram

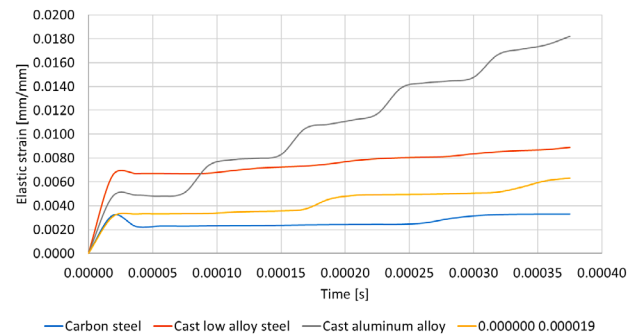


Figure 13. Average values of strain test

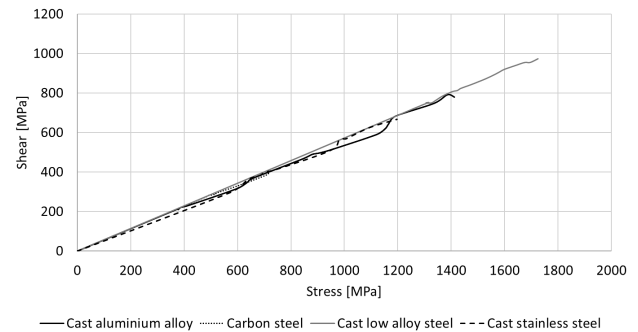


Figure 15. Shear vs. stress diagram

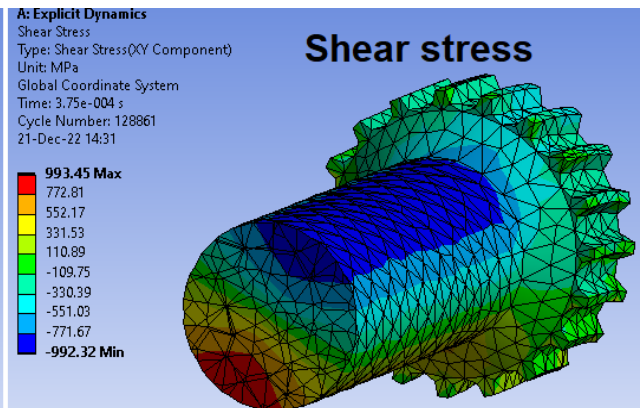
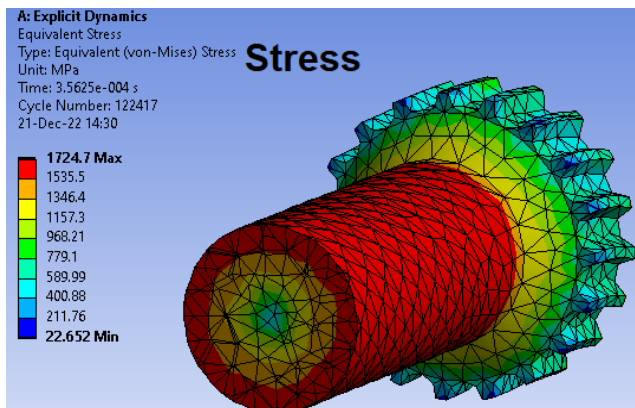


Figure 16. Cross-section of the part

To validate the shear stress, a cross-section has been plotted and presented in Figure 16. The cross-section of the part shows that the maximum values are obtained on the outer area of the part while in the centre area, the stress values retain their average values.

The shear stress diagram shows that the material with the highest shear value is low alloy steel, which also has the highest stress value. It should be noted that this material has the highest tensile and yield strength, making the shear level tolerable.

Figure 17 shows the deformation diagram as a function of time. During the complete rotation, the angular displacement of the material was about 16 mm at maximum for all materials tested. If we consider the safety factor of the material, we can obtain the part overall safety factor for each material, presented in Figures 18, 19, 20 and 21.

The safety factor can be defined as the ratio between the strength of the material and the maximum stress in the part and also gives an overview of how the material in the part would handle stresses and shows how the part would resist during deformation. This will give a better understanding at what area of a part, the stress is higher than the strength of the material [24].

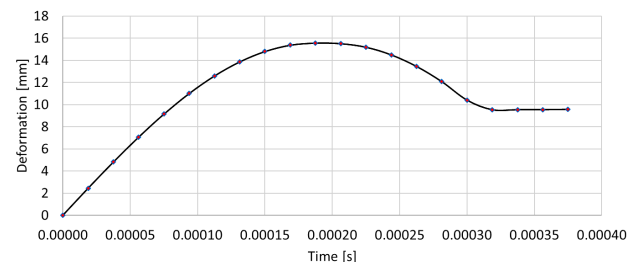


Figure 17. Deformation of the torsion bar in a 360 degree rotation

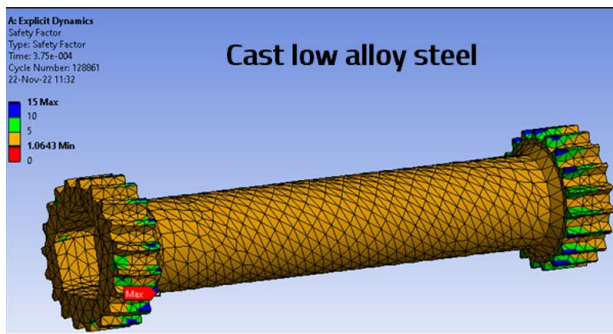


Figure 18. Safety factor for the cast low alloy steel

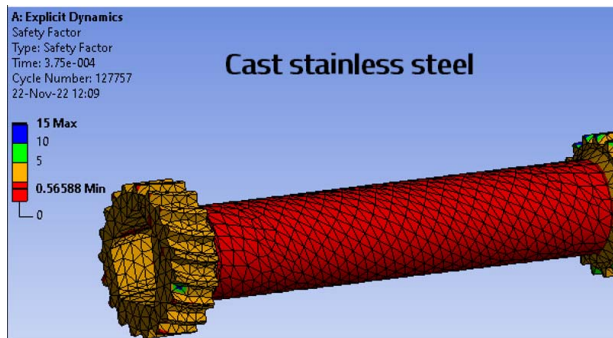


Figure 19. Safety factor for cast stainless steel

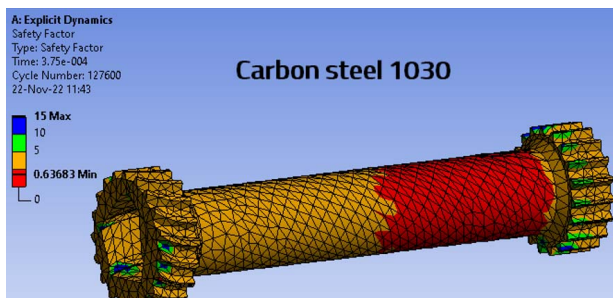


Figure 20. Safety factor for the carbon steel

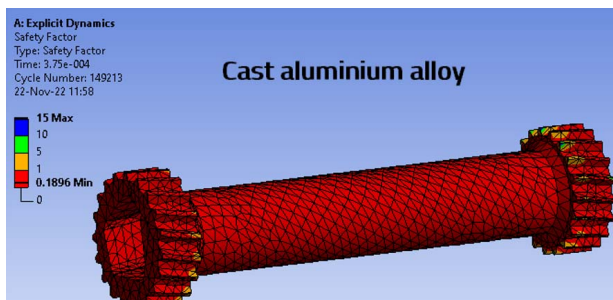


Figure 21. Safety factor for the cast aluminium alloy

The results of this analysis reveal that the material with the best safety factor (of at least 1) was the cast low alloy steel while the worst material is the cast aluminium alloy.

4. Conclusions

The results of this study show that each material has its advantages and disadvantages. The FEA results show that stiffer materials such as carbon steel and stainless steel have lower strain

and stress values, but also a lower safety factor of less than 1 in terms of durability. More resilient materials such as cast aluminium alloys and low alloy steel have twice the strain and stress values. However, only the low alloy steel has a safety factor of 1, indicating it would perform better under the given circumstances. The safety factor for the aluminium alloy shows that this material is too soft and would not perform as intended. The key function of torsion is to deform with a high elongation value during use and to release the seat belt after impact. In addition, the material must withstand stress during deformation to avoid shear stresses. If we consider the cost, the mass of the part and the overall performance of the material, the best material to use in this case would be low alloy cast steel.

References

- [1] V. Gupta, R. Menon, S. Gupta, A. Mani, I. Shanmugavelu, J. Kossar, Improved occupant protection through advanced seat design, in Proceedings of the 15th International Technical Conference on the Enhanced Safety of Vehicles, 13-16.05.1996, Melbourne, Australia, pp. 181-191.
- [2] M. Huang, Vehicle Crash Mechanics, CRC Press, Boca Raton, 2002.
- [3] A. Żuchowski, J. Jackowski, Analysis of properties of operation of the supporting equipment for the seat belts, Journal of KONES, Vol. 18, No. 1, 2011, pp. 697-704.
- [4] N. Yoganandan, A.M. Nahum, J.W. Melvin, Accidental Injury, Springer, New York, 2002, DOI: [10.1007/978-0-387-21787-1](https://doi.org/10.1007/978-0-387-21787-1)
- [5] N. Iovănescu, System of motor vehicle safety belt design elements and case study, Annals of the Faculty Engineering Hunedoara, Vol. 9, No. 3, 2011, pp. 247-253.
- [6] A.K. Abbas, A.F. Hefny, F.M. Abu-Zidan, Seatbelts and road traffic collision injuries, World Journal of Emergency Surgery, Vol. 6, 2011, Paper 18, DOI: [10.1186/1749-7922-6-18](https://doi.org/10.1186/1749-7922-6-18)
- [7] M.L. Brumbelow, B.C. Baker, J.M. Nolan, Effects of seat belt load limiters on driver fatalities in frontal crashes of passenger cars, in Proceedings of the 20th International Technical Conference on the Enhanced Safety of Vehicles, 18-21.06.2007, Lyon, France, Paper 07-0067.
- [8] L. D'Aulerio, G. Whitman, L. Sicher, A. Cantor, M. Markushewski, Forensic performance analysis of load-limiting devices in automotive seat belt retractors, Journal of Forensic Sciences, Vol. 64, No. 3, 2019, pp. 754-764, DOI: [10.1111/1556-4029.13955](https://doi.org/10.1111/1556-4029.13955)

- [9] R.A. DeMillo, W.M. McCracken, R.J. Martin, J.F. Passafiume, *Software Testing and Evaluation*, Benjamin-Cummings, San Francisco, 1987.
- [10] S. Tebby, E. Esmailzadeh, A. Barari, Methods to determine torsion stiffness in an automotive chassis, *Computer-Aided Design and Applications*, Vol. PACE, No. 1, 2011, pp. 67-75, DOI: [10.3722/cadaps.2011.PACE.67-75](https://doi.org/10.3722/cadaps.2011.PACE.67-75)
- [11] K. Khannukar, V. Kallannavar, B.S. Manjunath, Dynamic analysis of automotive chassis using FEA, *International Research Journal of Engineering and Technology*, Vol. 2, No. 9, 2015, pp. 2165-2170.
- [12] H.-s. Kim, Y.-s. Lee, S.-m. Yang, H.Y. Kang, Structural analysis on variable characteristics of automotive seat frame by FEA, *International Journal of Precision Engineering and Manufacturing-Green Technology*, Vol. 3, No. 1, 2016, pp. 75-79, DOI: [10.1007/s40684-016-0010-x](https://doi.org/10.1007/s40684-016-0010-x)
- [13] M. Pisaturo, A. Senatore, Simulation of engagement control in automotive dry-clutch and temperature field analysis through finite element model, *Applied Thermal Engineering*, Vol. 93, 2016, pp. 958-966, DOI: [10.1016/j.applthermaleng.2015.10.068](https://doi.org/10.1016/j.applthermaleng.2015.10.068)
- [14] S.R. Wu, J. Cheng, Advanced development of explicit FEA in automotive applications, *Computer Methods in Applied Mechanics and Engineering*, Vol. 149, No. 1-4, 1997, pp. 189-199, DOI: [10.1016/S0045-7825\(97\)00074-1](https://doi.org/10.1016/S0045-7825(97)00074-1)
- [15] M. Pervaiz, S. Panthapulakkal, Birat KC, M. Sain, J. Tjong, Emerging trends in automotive lightweighting through novel composite materials, *Materials Sciences and Applications*, Vol. 7, No. 1, 2016, pp. 26-38, DOI: [10.4236/msa.2016.71004](https://doi.org/10.4236/msa.2016.71004)
- [16] F. Czerwinski, Current trends in automotive lightweighting strategies and materials, *Materials*, Vol. 14, No. 21, 2021, paper 6631, DOI: [10.3390/ma14216631](https://doi.org/10.3390/ma14216631)
- [17] R.B. Kumbhar, C.R. Sonawane, P.N. Abhyankar, An overview of disarray in finite element analysis of composite torsion bar, *International Journal of Scientific Research in Science, Engineering and Technology*, Vol. 1, No. 6, 2015, pp. 59-62, DOI: [10.32628/IJSRSET151595](https://doi.org/10.32628/IJSRSET151595)
- [18] P.C. Kohnke, ANSYS, in C.A. Brebbia (Ed.), *Finite Element Systems*, Springer, Berlin, 1982, pp. 19-25, DOI: [10.1007/978-3-662-07229-5_2](https://doi.org/10.1007/978-3-662-07229-5_2)
- [19] Ansys material database, available at: <http://www.ansys.com/products/materials/materials-data-for-simulation>, accessed: 05.10.2022.
- [20] Fastmarkets, available at: <https://www.fastmarkets.com/commodity-price/aluminum-alloy-319-1-delivered-midwest-mb-al-0041>, accessed: 05.10.2022.
- [21] B.H. Liebman, Safeguards, China, and the price of steel, *Review of World Economics*, Vol. 142, No. 2, 2006, pp. 354-373, DOI: [10.1007/s10290-006-0071-y](https://doi.org/10.1007/s10290-006-0071-y)
- [22] P. Pawar, R. Ballav, A. Kumar, Finite element method broach tool drilling analysis using explicit dynamics ANSYS, *International Journal of Modern Manufacturing Technologies*, Vol. 8, No. 2, 2016, pp. 54-60.
- [23] A. Taub, E. De Moor, A. Luo, D.K. Matlock, J.G. Speer, U. Vaidya, Materials for automotive lightweighting, *Annual Review of Materials Research*, Vol. 49, 2019, pp. 327-359, DOI: [10.1146/annurev-matsci-070218-010134](https://doi.org/10.1146/annurev-matsci-070218-010134)
- [24] M. Badalassi, L. Biolzi, G. Royer-Carfagni, W. Salvatore, Safety factors for the structural design of glass, *Construction and Building Materials*, Vol. 55, 2014, pp. 114-127, DOI: [10.1016/j.conbuildmat.2014.01.005](https://doi.org/10.1016/j.conbuildmat.2014.01.005)